

# Immune profiling of melanoma tumors reflecting aggressiveness in a preclinical model

Sotirios P. Fortis<sup>1</sup> · Louisa G. Mahaira<sup>1</sup> · Eleftheria A. Anastasopoulou<sup>1</sup> · Ioannis F. Voutsas<sup>1</sup> · Sonia A. Perez<sup>1</sup> · Constantin N. Baxevanis<sup>1</sup>

Received: 23 March 2017 / Accepted: 23 August 2017 / Published online: 4 September 2017  
© Springer-Verlag GmbH Germany 2017

**Abstract** Melanoma, like most solid tumors, is highly heterogeneous in terms of invasive, proliferative, and tumor-initiating potential. This heterogeneity is the outcome of differential gene expression resulting from conditions in the tumor microenvironment and the selective pressure of the immune system. To investigate possible signatures combining immune-related gene expression and lymphocyte infiltration, we established a preclinical model using B16.F1-derived clones, in the context of melanoma aggressiveness. Combinatorial analyses revealed that tumors concomitantly expressing low levels of *Tnf-α*, *Pd-1*, *Il-10*, *Il-1ra*, *Ccl5*, *Ido*, high *Il-9*, and with low infiltration by CD45<sup>+</sup>, CD3<sup>+</sup>, CD4<sup>+</sup> and CD8<sup>+</sup> cells and a high CD4<sup>+</sup>:CD8<sup>+</sup> T cell ratio exhibited the most aggressive growth characteristics. Overall, these results support the notion that the intratumoral immunologic network molds aggressive melanoma phenotypes.

**Keywords** Melanoma · Heterogeneity · Aggressiveness · Immune signature · TILs

## Abbreviations

ARG	Arginase
CCL5	Chemokine (C–C motif) ligand 5
IDO	Indoleamine 2,3-dioxygenase

**Electronic supplementary material** The online version of this article (doi:10.1007/s00262-017-2056-1) contains supplementary material, which is available to authorized users.

✉ Constantin N. Baxevanis  
baxevanis@ciic.gr

<sup>1</sup> Cancer Immunology and Immunotherapy Center, “Saint Savas” Cancer Hospital, 171 Alexandras Avenue, 11522 Athens, Greece

IL	Interleukin
IL-1Ra	IL-1 receptor antagonist
NKs	Natural killer cells
PD1	Programmed cell death protein 1
PD-L1	PD-1 ligand
TGF-β	Transforming growth factor beta
TILs	Tumor infiltrating lymphocytes
TNF-α	Tumor necrosis factor-alpha
Tregs	T regulatory cells
VEGF	Vascular endothelial growth factor

## Introduction

Melanoma, like most solid tumors, is highly heterogeneous, regarding invasive, proliferative, and tumor-initiating potential [1–3]. Heterogeneity is the result of differential gene expression under the pressure of tumor microenvironment and hosts’ immune system [4]. According to recent reports [3, 5], highly genetic instability in melanoma along with reciprocal interactions between tumor cells and elements of the immune system promotes melanoma plasticity and thus therapeutic resistance.

The previous reports have shown that tumors recruit distinct cell populations at the tumor microenvironment, some with immunosuppressive function, creating a sensitive balance between the “friends and foes” of the immune system. An increasing number of studies in melanoma, colon cancer, breast cancer, and other types report a significant correlation of tumor infiltrating lymphocytes (TILs) (e.g. CD3<sup>+</sup>, CD4<sup>+</sup>, and CD8<sup>+</sup>) with a positive disease outcome or lower risk of death in cancer patients, independently of other classical prognostic factors [6].

Melanoma microenvironment encompasses immune subpopulations and cancer cells communicating via secreting

molecules which may act as attractors, activators, immune suppressors, or supporters of tumor escape mechanisms. Among these messenger molecules are numerous enzymes, cytokines, and chemokines. These immune messengers either produced by tumor cells or surrounding tumor microenvironment possess pleiotropic functions depending on their context [7, 8].

The profile of melanoma tumor has been extensively investigated [8]; however, many issues remain obscure regarding development and progression. The continuously altering immune microenvironment, often described across various melanoma subtypes, correlating with different prognosis and clinical outcomes, ascribes a functional role to immune-related molecules as candidates for potentially valuable signatures [9, 10]. Many studies have identified several signatures in melanoma relating not only mutations in key molecules associated with signal transduction, but also distribution and architecture of immune cell subpopulations in tumor microenvironment [11]. It is noteworthy to mention that several reports have described signatures entailing a large number of genes related to immune-messenger mediators with a substantial role in melanoma progression [10]. Recent studies have underlined the prognostic significance of signatures involving immune-related gene expression patterns [12, 13]. The established diagnostic biomarkers focus mainly on alterations or/and deregulations of melanocytes rather than melanoma itself. However, considering the interactions within the tumor microenvironment, panels employing more than a single marker may be more informative in the context of prognosis and prediction [14].

Melanoma growth characteristics are of great prognostic significance, since histological assessment and more specifically Breslow tumor thickness are used for melanoma diagnosis and serve as a prognostic biomarker [15]. Given the limited number of studies simultaneously assessing immune cell infiltration, growth characteristics, and immune-related genes, our aim was to establish a preclinical model reflecting melanoma heterogeneity, considering the complicated and multifactorial interplay among tumor microenvironment, which promotes aggressiveness. Taking into account the remarkable melanoma heterogeneity, often driven by the adaptive plasticity under the pressure of the immune system [4, 16], we decided to investigate possible signatures combining immune-related gene expression (i.e., TGF- $\beta$ , TNF- $\alpha$ , CCL5, IL-9, IL-10, IL-1Ra, PD-1, IDO, and ARG) and lymphocytes infiltration, to characterize melanoma aggressiveness.

## Materials and methods

### Cell lines and generation of clones

B16.F1 and B16.F10 melanoma murine cell lines were obtained by ATCC (American Type Culture Collection) and

cultured in DMEM (Dulbecco's Modified Eagle Medium) (Biochrom), supplemented with 10% FBS (Biochrom) and 1 $\times$  antibiotic–antimycotic (Life Technologies), designated as complete medium (CM). Cultures were kept always in logarithmic phase of growth and sub-cultured using treatment for 2 min with Trypsin 0.25%-EDTA (Ethylene-diaminetetraacetic acid) solution (Life Technologies). Clones were generated from B16.F1 cell line, applying the limiting dilution assay, by seeding 1 cell/well in 96-well plates in CM. Media were replenished every 2 days. The total number of clones was 22, in compliance with the estimated numbers by the likelihood equations of this assay. We randomly selected four clones (#13, #15, #17, and #22) exhibiting notable differences regarding proliferation rates in vitro, cell morphology, anchorage independence, and melanin production. Most recent work from our laboratory has confirmed this heterogeneity in the above clones by the in vitro expression pattern of several genes (*Igf2bp1*, *Ptma*, *c-Myc*, *Bcl2*, *Melan-A*, and *Mitf*) [17].

### Animals

All protocols were reviewed by the competent authority of our institution, for compliance with the Greek and European regulations on Animal Welfare and with Public Health Service recommendations. Female C57BL/6 mice aged 6–8 weeks old (Hellenic Pasteur Institute, Greece) were maintained in pathogen-free conditions in an animal facility, on an inverse 12:12-h light–dark cycle with ad libitum access to water and food. Animals ( $n = 5$ ) were randomly assigned to receive  $5 \times 10^5$  cells of each clone, clone mixtures, or parental cell lines in 100  $\mu$ l Phosphate Buffered Saline (PBS) inoculation, by subcutaneous injection on their flank. Tumor growth was monitored daily and after being palpable, caliper was used to estimate growth by measuring the two diameters and extracting the orthogonal mean:  $(d1 + d2)/2$ . Mice ( $n = 35$ ) were inoculated with melanoma cells on day 0, and by the time, the first mouse developed a tumor slightly exceeding 2 cm in diameter (orthogonal mean) (16-day postinoculation), all animals were euthanized by CO<sub>2</sub> inhalation and tumor masses were recorded. Subsequently, tumors were homogenized in ice cold PBS 1 $\times$  solution and passed through a 70- $\mu$ m nylon cell strainer (BD Biosciences). Single cell suspensions were used to assess antigen expression by FACS analysis or gene expression by qRT-PCR.

### RNA extraction and qRT-PCR

RNA was extracted from cell cultures or tumor cells using NucleoSpin RNA II kit (Macherey–Nagel GmbH&Co) according to instructions. rDNase treatment was performed to remove any residual genomic DNA. Total RNA (1  $\mu$ g)

was reverse transcribed using PrimeScript Reverse Transcriptase (TaKaRa, Bio Inc.) and random hexamer oligonucleotides (Invitrogen, Life Technologies). Quantitative RT-PCR (qPCR) was performed on a Rotor-Gene 3000 (Corbett Research, Life Technologies, USA), in a 20- $\mu$ L reaction using 200-ng cDNA solution, KAPA SybrFast qPCR kit (KapaBiosystems), and 200 nMol of specific primers (synthesized by VBC Biotech Service, Austria). Primers' sequences are presented in the Supplementary Table s1. DDCT method was used for data analysis and melting curve analysis for specificity of gene expression levels. Gapdh (Glyceraldehyde 3-phosphate dehydrogenase) mRNA levels served as internal normalization gene and the in vitro growing B16.F1 cell line as reference sample.

### Flow cytometry and quantification of absolute cell numbers

Absolute counts of TILs were performed using TrueCount tubes (Becton–Dickinson), according to the manufacturer's instructions. In brief, tumors were excised, weighed, and homogenized in cold FACS buffer (to final concentration 1 mg of tumor/ml). One hundred microliters of this single cell suspension was stained for 15 min at room temperature with pre-titrated combinations of anti-CD45–PerCP/Cy5.5, anti-CD4–APC, anti-CD3–FITC, and anti-CD8–PE (eBioscience), and analyzed by flow cytometry on BD FACS Canto II (BD Biosciences, USA) using FlowJo 8.7 (TreeStar Inc., USA) software.

### Statistical analysis

Statistical analyses were performed by GraphPad Prism v.5.0 software, using Spearman's correlation with 95% confidence interval, Fisher's exact test and Mann–Whitney *t* test, accordingly. *p* values <0.05 were considered statistical significant.

## Results

### Establishment of tumors with diverse biologic characteristics from the same paternal cell line

Our goal was to create a preclinical melanoma model, using the parental B16.F1 murine melanoma cell line, reflecting melanoma heterogeneity. To this end, we generated and randomly selected 4 out of 22 clones from this cell line, which exhibited significant differences regarding their in vitro characteristics (morphology, cell growth, anchorage independence, and melanin production), cancer-related gene expression profiles, and in vivo growth potential [17].  $5 \times 10^5$  viable cells of each clone (#13, #15, #17, and #22)

separately or in mixtures ( $1.25 \times 10^5$  cells from each of the four clones), or an equal number of cells from the B16.F1 and the B16.F10 cell lines (the latter is derived from in vivo passaging of the paternal B16.F1 [18]), were injected subcutaneously into syngeneic C57Bl/6 mice ( $n = 5$  per group) and growth was monitored as described in Materials and methods section. Three of thirty-five animals injected (one animal in each of the groups inoculated with clone #13, clone #15, and clone mixtures) died on day 14 and, therefore, were not included in the analyses. Figure 1a shows the growth kinetics of tumors (orthogonal mean of diameters) generated by each clone/line, with B16.F10-derived tumors growing faster and clone #13 generating the slowest growing tumors. On 16th day, animals were sacrificed, the final diameter for each tumor was recorded (Fig. 1a, bi), and then, tumors were excised and weighted (Fig. 1bii). Higher tumor mass represents more rapidly growing (more aggressive) tumors, with tumors derived from clones #13, #15, and #22 being the less aggressive. Since one of the most relevant prognostic factors in melanoma is the invasiveness of tumor, we also compared the tumors generated from the different clones/lines according to their ratio of mass/diameter as an invasiveness indicator. In general, melanoma tumors are classified based on two fundamental criteria: (a) mitotic index which represents proliferation rates of cells and (b) Breslow thickness and radial or vertical growth which characterize invasive melanoma as superficial or nodular [19]. Based on that, we decided to use final tumor mass and the ratio mass/diameter (measured at the endpoint) to reflect these two criteria in our preclinical model [17]. As depicted in Fig. 1biii, there was a high heterogeneity among the different clones/lines, with B16.F10 and clone #17 generating mostly highly invasive tumors and clone #22-derived tumors growing superficially. In all cases, there were statistically significant differences among tumors generated by the different clones and cell lines regarding diameter, mass, and the ratio mass/diameter (Supplementary Table s2). These differential growth patterns are indicative of melanoma heterogeneity reflected in our model.

To better substantiate the heterogeneity of the melanoma tumors generated in our model, we investigated a number of immune-related parameters, including immunoregulatory molecules and immune cell infiltration, of the tumors generated from the different clones/lines. Thus, apart from the differences in growth characteristics, there were significant differences in gene expression (mRNA levels) of several immune-related factors. Figure 2a shows intragroup as well as intergroup variations in the relative mRNA expression levels of *Arg*, *Tgf- $\beta$* , *Il-10*, *Ido*, *Pd-1*, *Il1-ra*, *Il-9*, *Tnf-a*, and *Ccl5*. Comparisons (*p* values) among groups of tumors derived from the different clones and lines are presented in Supplementary Table S3. An analogous situation was found when classifying the tumors as high or low expressers based

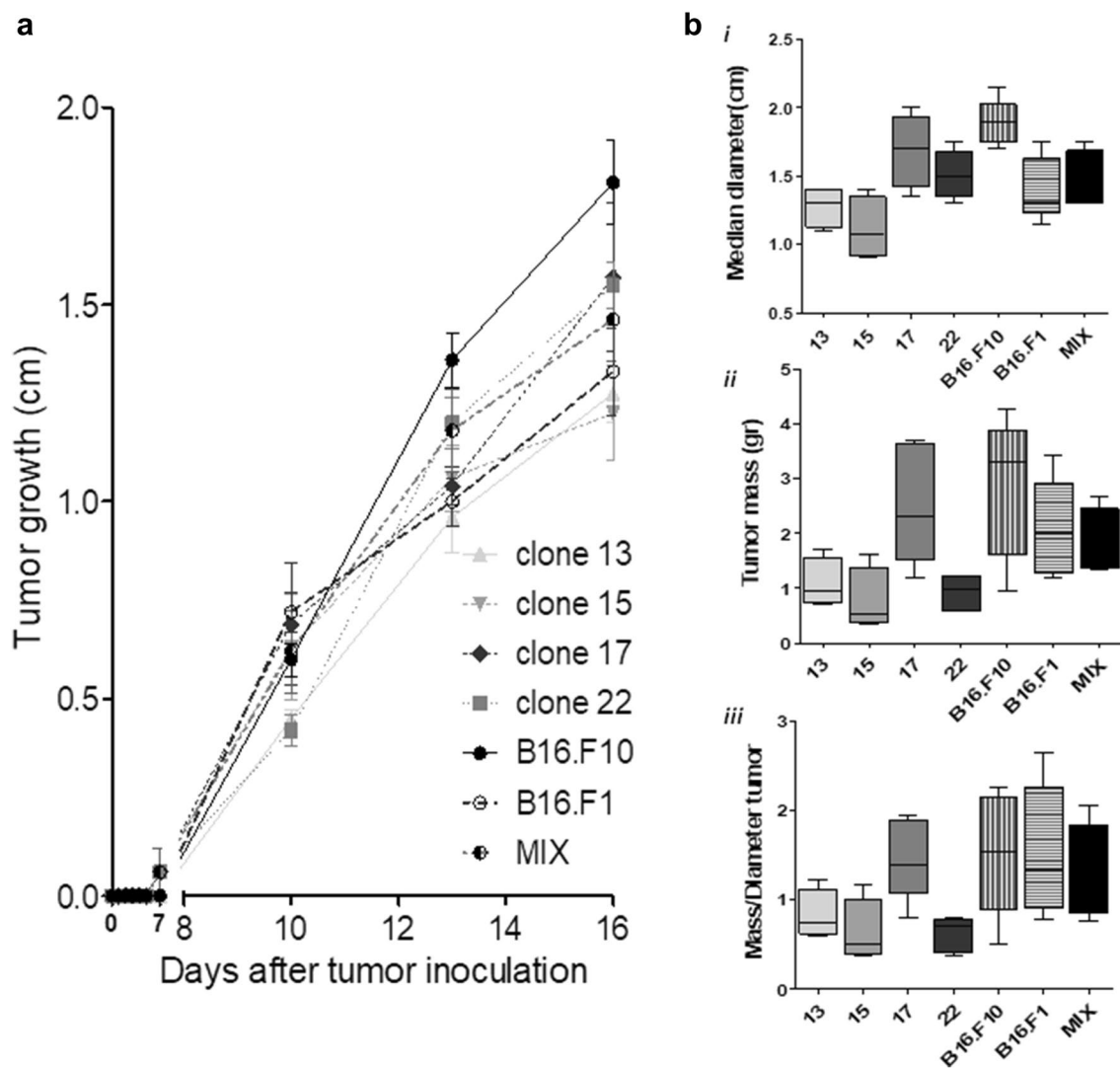


**Fig. 1** Establishment of tumors with diverse growth characteristics. **a** Growth curves presenting the orthogonal mean (cm) of tumors generated by all clones/lines and mixtures thereof (mix). **b** Box plots present final diameter (**i**), mass (**ii**), and mass/diameter (**iii**) for each

tumor ( $n = 5$  mice per clone/line or mix). Note that by day 14, one animal from each of the groups inoculated with clones #13, #15, and mix and dried, and therefore, analyses in these particular groups (day 16) included 4 animals

on whether they expressed the gene of interest at levels above or below, respectively, the median value measured in all tumors induced by either the clones or the cell lines. Thus, as shown in Fig. 2b, there was a significant variance in the levels of expression of a certain gene among groups. In addition, there was a wide range of variation in the expression of the genes analyzed by tumors induced by the same clone or line.

Since tumor infiltration by immune cells is emerging as a very useful prognostic marker in many cancer types, including melanoma, we also investigated the heterogeneity of immune cell infiltration of tumors generated from the different clones or lines. Figure 2c shows the density of tumor infiltration by  $CD45^+$  (total leukocytes),  $CD3^+$ ,  $CD4^+$  and

$CD8^+$  T cells, expressed as number of cells per gr of tumor, as well as the ratio of  $CD4/CD8$ . There were statistically significant differences among tumors generated by the different clones and lines (see also Supplementary Table s4). Tumors derived from clone #13 exhibited high heterogeneity in their degree of infiltration by all subpopulations examined. Significant heterogeneity was also observed within other groups of tumors, although to a lesser extent.

Taken together, our results generated from the experimental model presented herein demonstrate a great heterogeneity in terms of growth, genomic profiling, and immune infiltration among tumors from different clones or lines, and more intriguing among tumors derived from the same clone or line. Thus, in the following sections, all tumors

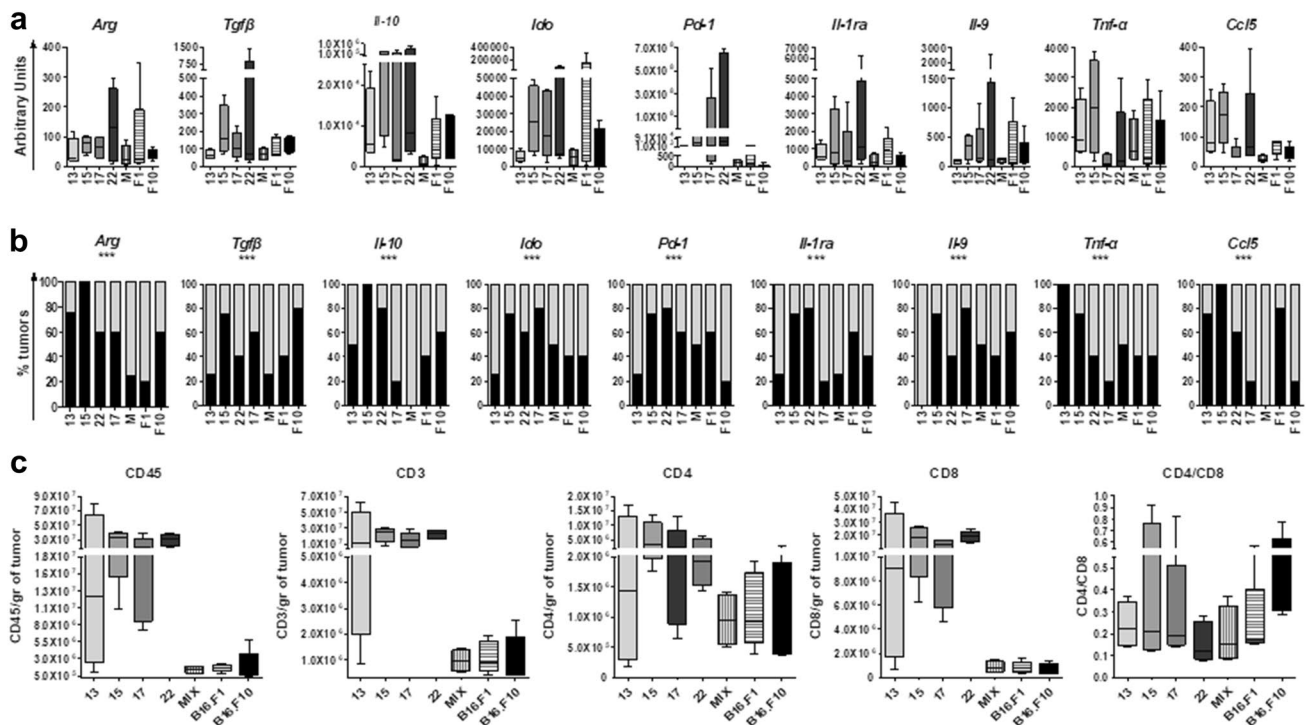


**Fig. 2** Gene expression and infiltration of tumors generated by clones and cell lines. **a** Graph shows box plots with Whiskers from minimum to maximum mRNA levels of all genes studied (Arbitrary Units). Each box plot presents tumors generated by each clone/line. **b** Percentages of tumors generated by each clone/line exhibiting high

(above the median of all values) (in black) or low (equal or below median) (in grey) levels of gene expression. **c** Box plots depict density of infiltration by CD45<sup>+</sup> (total leukocytes), CD3<sup>+</sup>, CD4<sup>+</sup> and CD8<sup>+</sup> T cells, expressed as number of cells per gram of tumor mass, as well as the ratio of CD4/CD8. (Number of mice: See Fig. 1b legend)

were grouped and analyzed based on their characteristics as outlined above, and independently of the clone/line used for their generation.

**Tumor growth characteristics are differentially correlated with different immune-related genes**

Next, we analyzed the levels of expression of immune-related genes in relation to tumor growth characteristics, i.e., mass and mass/diameter, in the total number of tumors ( $n = 32$ ). As shown in Fig. 3a, *Il-10* and *Ccl5* mRNA levels exhibited a direct, negative, correlation with tumor mass ( $p = 0.0008$  and  $p = 0.0009$ , respectively) and mass/diameter ratio ( $p = 0.0009$  and  $0.0073$ , respectively). Then, tumors were grouped in fast vs slow growing [i.e., high (H) mass vs low (L) mass based on whether their mass was above or below (high or low, respectively) the median value for all tumors], and in invasive vs superficially growing (i.e., H vs L mass/diameter). It has to be mentioned that tumors with H or L mass were the same with those exhibiting H or L mass/diameter. Thus, the subgroup analyses apply to both groups, even in the absence of direct values correlation. We found that less (L) aggressive tumors expressed higher

levels of *IL-10*, *IL-1ra*, *Tnf- $\alpha$* , and *Ccl5*, but lower levels of *IL-9*, compared to the fast proliferating (H) invasive ones (Fig. 3b, c).

**Immune-cell infiltration varies among tumors with different growth characteristics**

Taking into account the observed heterogeneity of inter- and intra-group analyses in our model, we decided to also analyze the immune cell infiltration in the total number of tumors of all clones. As depicted in Fig. 4, strong negative correlations were observed between infiltration by CD45<sup>+</sup>, CD3<sup>+</sup>, CD8<sup>+</sup>, and CD4<sup>+</sup> cells and tumor mass (Fig. 4a). As expected, we observed similar correlations when comparing with mass/diameter (Fig. 4b). The ratio of CD4<sup>+</sup>/CD8<sup>+</sup> positively correlated with mass and mass/diameter ratio. These results show that more aggressive tumors are characterized by less infiltration by immune cell populations. This finding was more profound when CD8<sup>+</sup> T cell infiltration was analyzed and was supported by the fact that predominance of CD8<sup>+</sup> cells in the T lymphocyte compartment, as represented by the lower CD4<sup>+</sup>/CD8<sup>+</sup> ratio, was found to be robustly correlated with less aggressive tumors.



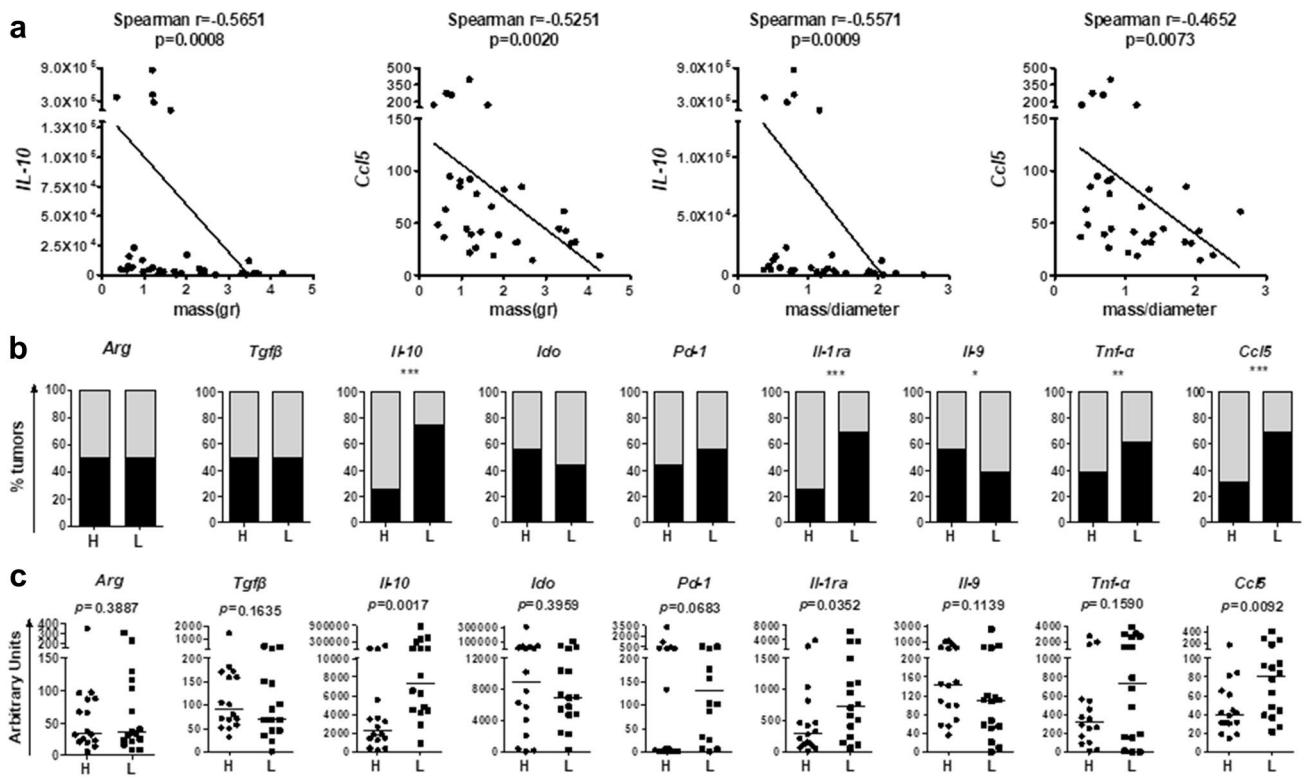


**Fig. 3** Correlations of gene expression and growth characteristics. **a** Grouped analyses of gene expression, in relation to mass and mass/diameter ratio. All tumors generated by all clones/lines ( $n = 32$ ) were included. *Il-10* and *Ccl5* mRNA levels negatively correlated to mass and mass/diameter ratio. **b** *Graphs* display percentages of tumors

exhibiting more or less aggressive phenotype (i.e., high (H) mass vs low (L) mass and high mass/diameter vs low ratio). Tumors with H or L mass were the same with those exhibiting H or L mass/diameter ratio. **c** *Scatter dot plots* present individual tumors exhibiting more (H) or less (L) aggressive phenotype (H;  $n = 16$ , L;  $n = 16$ )

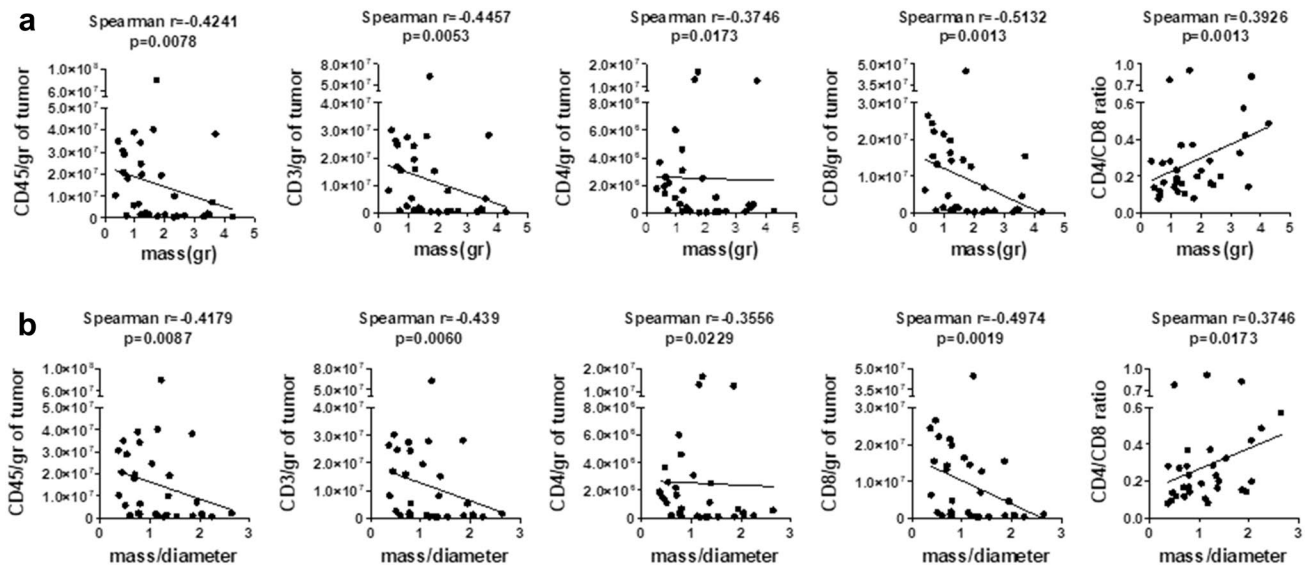


**Fig. 4** Correlations between infiltration by immune cell populations and tumor growth. Depicted are correlations of infiltration by CD45<sup>+</sup>, CD3<sup>+</sup>, CD8<sup>+</sup>, CD4<sup>+</sup> T cells, and ratio CD4/CD8 with tumor mass (gr) (a) or mass/diameter (b) ( $n = 32$ )

### Correlations between tumor infiltrating immune cell populations and immune-related genes

Given that tumors express immune-related factors [20, 21], our next goal was to test whether gene expression levels measured above (Fig. 2) were influenced by and correlated with tumor immune-cell infiltration. By analyzing all tumors, irrespectively of their origin, according to CD45<sup>+</sup> T cell infiltration (similar results were obtained from analyses based on CD4<sup>+</sup> or CD8<sup>+</sup> infiltrating populations, data not shown) in relation to mRNA levels for the gene of choice, we were able to show a statistically significant positive correlation with *Ccl5* ( $p = 0.0059$ ), *Arg* ( $p = 0.0070$ ), *Ido*

( $p = 0.0341$ ), *IL-1Ra* ( $p = 0.0074$ ), *Pd-1* ( $p = 0.0128$ ), and *IL-10* ( $p = 0.0347$ ) expression (Fig. 5). On the contrary, no correlation ( $p > 0.28$ ) was observed between *Tgfb-1*, *Il-9* and *Tnf-a*, suggesting that these molecules were co-expressed by tumor and immune cells or that there is a variable functionality of infiltrating immune cells among different tumors, or both.

### Possible prognostic signatures

So far, we showed that single immune-related parameters, either as gene expression levels coding for immune factors or as infiltrating immune populations, are differentially related

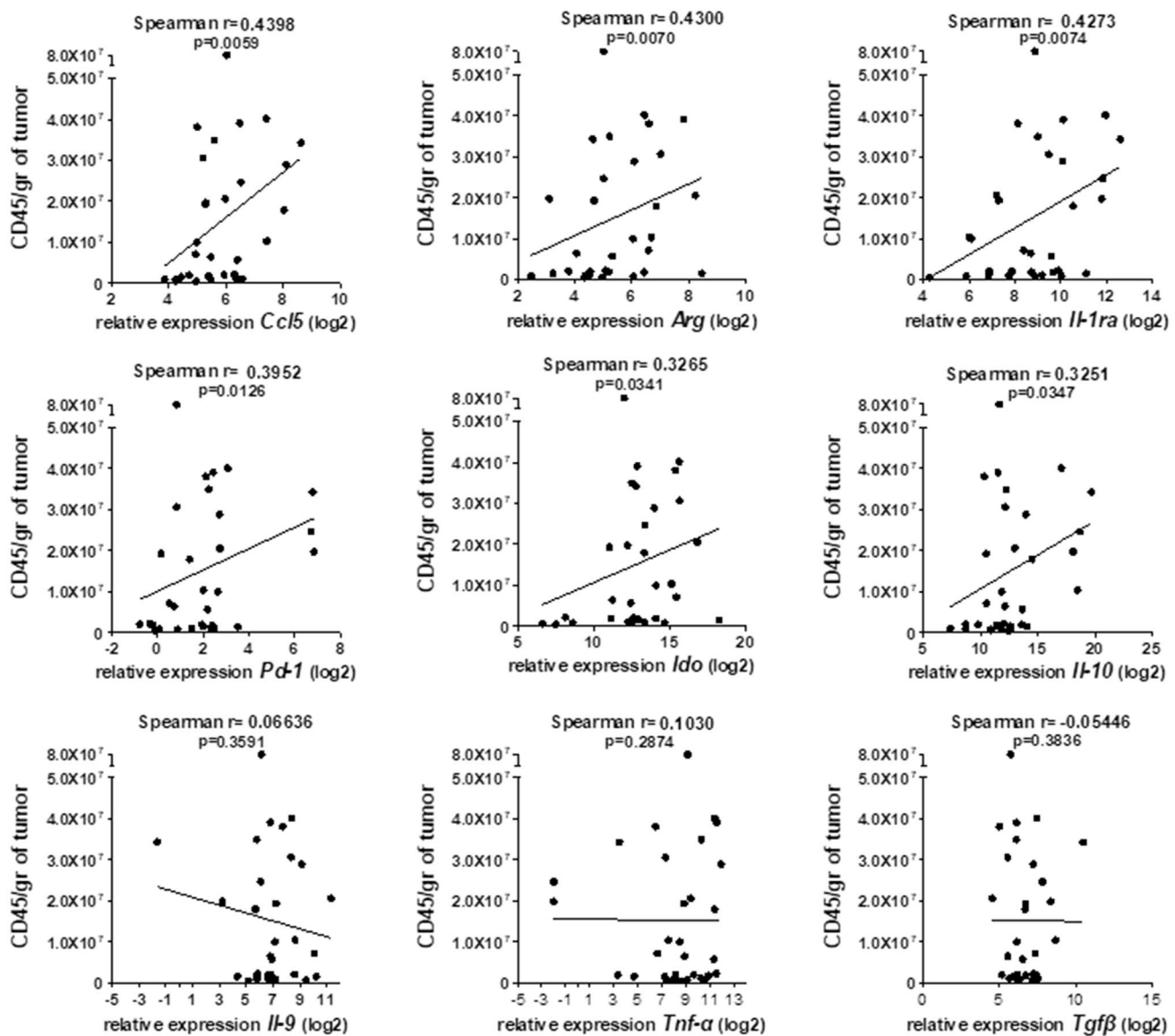


**Fig. 5** Correlations between tumor infiltrating CD45<sup>+</sup> cells and immune-related gene expression. *Graphs* display correlations between density of CD45<sup>+</sup> cell infiltration and logarithmic values (log<sub>2</sub>) of gene expression levels (mRNA, arbitrary units) ( $n = 32$ )

to the main prognostic markers of melanoma, i.e., growth rate and tumor depth (represented here as tumor mass and mass/diameter ratio, respectively). Thus, our next step was to combine several of these parameters, to obtain possible prognostic signatures.

Initially, we compared between the aggressiveness (i.e., mass and mass-to-diameter ratio) of the tumors generated by all clones/lines and their capacity to be high (H) or low (L)

expressers, as far as it concerns the levels of expression of the analyzed genes (Fig. 6a). The concomitant low expression of *Il-10* and *Il-1ra* was found to correlate with increased mass ( $p = 0.0006$ ; H expressers,  $n = 11$ ; L expressers,  $n = 12$ ). Low co-expression of *Il-10* and *Pd-1* was also correlated with increased mass ( $p = 0.0039$ , H,  $n = 10$ ; L,  $n = 10$ ), whereas low levels of *Il-10*, *Pd-1*, and *Il-1ra* correlated with increased mass ( $p = 0.0111$ ; H,  $n = 8$ ; L,  $n = 9$ ). By adding to this

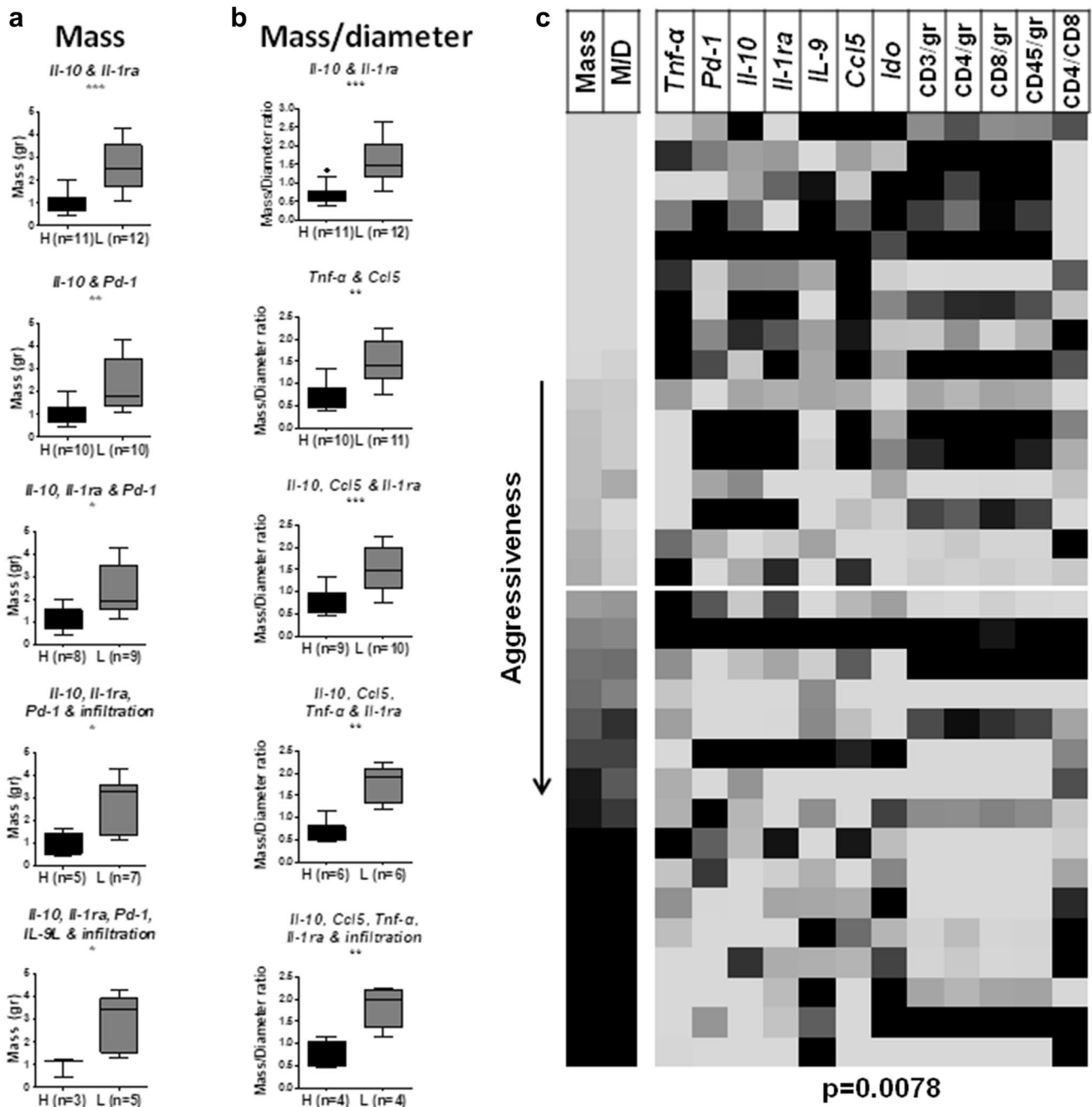


**Fig. 6** Possible prognostic signatures. *Box and Whisker plots* present concomitant expression levels of immune related genes and infiltration by CD8<sup>+</sup> T cells in respect to **a** mass and **b** mass/diameter. H, L = high or low levels of expression or infiltration, respectively. **c**

Heat map displaying all parameters analyzed (gene expression and tumor infiltration) in relation to aggressiveness (based on mass and mass/diameter ratio values) for all ( $n = 32$ ) tumors



three-gene analysis also the levels of CD8<sup>+</sup> cell infiltration, we also found that low levels of all four parameters correlated with increased mass ( $p = 0.0303$ , H,  $n = 5$ ; L,  $n = 7$ ). Considering *Il-9* gene expression as an additional parameter to our analysis, we showed that low levels of *Il-10*, *Pd-1*, and *Il-1ra*, along with high levels of *Il-9* and low CD8<sup>+</sup> T cell infiltration vs the reverse combination, namely high levels of *Il-10*, *Pd-1*, *Il-1ra*, low levels of *Il-9*, and high CD8<sup>+</sup> T cell infiltration, we were able to further discriminate between high and low aggressive tumors ( $p = 0.0357$ ).

We next followed a similar way of analyses combining the expression (H or L) of multiple immune parameters in relation to the mass/diameter ratio (Fig. 6b). Tumors concomitantly expressing low levels of *Il-10* and *Il-1ra* or *Tnf- $\alpha$*  and *Ccl5* were characterized by increased mass/diameter ratios ( $p = 0.0004$  and  $p = 0.0011$ , respectively). The combined low co-expression of three genes (*Il-10*, *Ccl5*, and *Il-1ra*) and four genes (*Il-10*, *Ccl5*, *Tnf- $\alpha$* , and *Il-1ra*) also strongly correlated with increased mass/diameter ratios ( $p = 0.0010$  and  $p = 0.0022$ , respectively). Finally, by adding to the four genes signature the CD8<sup>+</sup> T cell infiltration, we found that low levels of all five parameters characterized tumors with increased mass/diameter ratios ( $p = 0.0286$ ). It has to be mentioned that  $p$  values increased by adding more parameters to the analyses due to a substantial decrease in the number of tumors (see legend) fulfilling all the prerequisites in each category.

Finally, by constructing a heat map (Fig. 6c) of all parameters found to correlate, separately or in combinations, with growth rate (mass) and invasiveness (mass/diameter), we were able to define a signature strongly correlating with tumor aggressiveness: more aggressive tumors expressed lower levels of *Tnf- $\alpha$* , *Pd-1*, *Il-10*, *Il-1ra*, *Ccl5*, and *Ido*, higher *Il-9*, as well as lower infiltration by CD45<sup>+</sup>, CD3<sup>+</sup>, CD4<sup>+</sup>, and CD8<sup>+</sup> cells and a higher ratio of CD4/CD8 T cells ( $p = 0.0078$ ).

## Discussion

The large heterogeneity in the molecular landscape of melanomas led to the identification of biomarkers, associated with altered gene expression proposing diagnostic and prognostic significance [13]. However, cancer heterogeneity may also refer to diverse secretion of immune-suppressive enzymes and chemokines or inflammatory proteins along with the expression of their respective receptors. A complex network guided by the release of factors with opposing effects and the expression of immune checkpoints may regulate qualitatively and quantitatively cell interactions in tumor microenvironment which in turn may significantly impact immune evasion or immune recognition [22]. Hence, melanoma plasticity is a dynamic process under the control of the immune context.

B16-derived cell lines (e.g., B16-F1 and B16-F10) are quite heterogeneous containing clones which differ significantly in their metastatic properties. Despite these differences, they follow similar patterns of evolutionary selection processes in vivo which points to a common pathway of interactions among different subclones of the same tumor [23–26]. Such evolutionary processes provide a novel paradigm of tumor progression which is based on interactions with microenvironmental factors. Considering these observations and our most recent findings—which demonstrated a molecular signature in B16-F1-derived clones possibly associated with melanoma heterogeneity [17]—in the current study, by conducting experimentations with the same clones, we further explored melanoma growth in association with infiltrating immune cells and immune-related molecular profiles. By inoculating our B16-F1-derived clones, we generated a preclinical model which gave rise to melanoma tumors with differential growth characteristics, immune-related gene expression, and lymphocyte infiltration, thus reflecting melanoma heterogeneity. We observed great inter- and intra-group heterogeneity, which is in accordance with the previous results describing that highly heterogeneous tumor variants preexist in the B16 parental cell line [26]. In the previous studies, B16 melanoma cell populations have shown marked differences in their stability regarding their growth kinetics after passages in vivo or in vitro as polyclonal populations due to the presence of clones expressing heterogeneous growth [27]. In particular, cell lines established from B16, or B16-F1 tumors, were found to have a heterogeneous content of clones with different growth and metastatic potential. Notwithstanding, these cell lines when inoculated as polyclonal populations exhibited a homogeneous growth [13, 14, 24]. In the same lines, clonal subpopulations derived by limiting dilution from B16 or B16-F1 cell lines exhibited a highly heterogeneous growth; markedly, this heterogeneity in growth was to a great extent diminished when the same clones were cultured in mixtures to form a polyclonal population [28]. Our data are in line and extend these observations by demonstrating that the B16-F1 clones grew in vivo exhibiting heterogeneity presumably, as a result of their differential responses to a variety of selection procedures also including those induced by the immune microenvironment [16].

Our findings demonstrate intergroup broad spectrum heterogeneity in terms of growth and gene expression behavior among melanomas induced upon inoculation of clones derived from the same parental tumor cell line (i.e., the B16-F1). Notably, such heterogeneity in growth and gene expression was also found among melanomas induced by single clones, reflecting intragroup heterogeneity. In a previous report, Poste G et al. [28] have shown that in vitro cultured clones derived from the B16 cell line when inoculated in transplantable animals rapidly generated variants

with different metastatic properties. Because of the wide spectrum of the metastatic properties of the various subclones, their results indicated that the parental clone was genetically and phenotypically unstable. Given that tumor evolution is no longer considered as a cell-autonomous process [29], this instability may result from the development and gradual selection of tumor variants influenced by the tumor microenvironment. Importantly, the broad range of such inter- and intra- group diversities was diminished when tumors, independently of their origin (i.e., of the inducing clone), were grouped based on growth properties (i.e., high mass vs low mass). Accordingly, the majority of individual clones which yielded tumors with similar growth phenotypes also induced similar cell and molecular immune profiles in these tumors. Because of this marked heterogeneity, it was obvious that analyses of melanomas induced by each single clone separately would provide elusive information. Therefore, our experiments comprising of and comparing between tumor groups bearing limited range of growth, irrespective of the inducing clone, provided useful insights regarding progression of melanomas relative to their genomic and immune markers.

In detail, we investigated the expression of TGF- $\beta$ , TNF- $\alpha$ , CCL5, IL-9, IL-10, IL-1Ra, PD-1, IDO, and ARG, all of which have been reported to participate in crucial immune interactions in tumor microenvironment [30–34]. Given that these interactions shape tumor growth, we correlated gene expression patterns with tumor growth characteristics. Our findings showed that combined augmented expression of *Il-10*, *Il-1ra*, *Pd-1*, and CD8<sup>+</sup> infiltration along with low levels of *Il9* was associated with low tumor mass. Moreover, tumors with the most aggressive phenotype, reflected by high values of mass/diameter ratio, were characterized by concomitant low expression of *Il-10*, *Il-1ra*, *Tnf- $\alpha$* , *Ccl5*, and low CD8<sup>+</sup> infiltration.

Our proposed signature suggests that low levels of *Il-10* correlate with increased tumor growth and aggressiveness. IL-10 is a cytokine with pleiotropic effects in immunoregulation and inflammation and its production correlated with important prognostic implications for the transition from melanoma in situ to invasive and metastatic melanoma [35]. Despite the immunosuppressant role of IL-10, recent studies, in line with our results, show that this cytokine can induce strong antitumor responses in the presence of CD8<sup>+</sup> T cells [36]. It has been described that CD8<sup>+</sup> T cells can engage adaptive and innate immune responses, leading to tumor regression in a preclinical model of melanoma [37]. Considering the cytotoxic effect of CD8<sup>+</sup> T cells [6, 38], it is noteworthy to mention that low levels of *Il-10* coincide with low CD8<sup>+</sup> tumor infiltration allowing the establishment of melanoma tumors of increased aggressiveness.

As far as IL-1Ra is concerned, its role has been studied in colon and melanoma cancers [32]. Studies in preclinical

models have demonstrated that IL-1Ra hinders tumor progression and promotes antitumor responses in established melanoma tumors [39]. Beside this, it has been described to block VEGF function, inhibiting growth and metastasis in a preclinical model [33]. In line with these reports, we found that low levels of *Il-1ra* are associated with high mass and tumor aggressiveness, further supporting the beneficial effect of this molecule.

IL-9 exhibits multifaceted actions by negatively or positively regulating immune responses [40]. Moreover, recent reports suggest that IL-9 promotes survival and activates antitumor T cell responses [41]. On the other hand, it has been described that IL-9 modulates tumor progression by enhancing the immunosuppressive function of Tregs [42]. In agreement with this, elevated levels of *Il-9* characterize tumors with high mass in the preclinical model described herein.

The signature proposed in the current study, correlated low levels of *Pd-1* to increased tumor growth rate, which seems to be contradictory to the previous reports [43]. PD1 is present on the surface of activated lymphocytes and is implicated in tumor escape mechanisms through PD-1/PD-L1 axis, leading to T cell inactivation [44]. Therefore, we hypothesize that low levels of *Pd-1* observed in our model may be due to the low number of tumor infiltrating lymphocytes.

The previous studies have ascribed an immunosuppressive role to CCL5 by showing that this chemokine attracts Tregs intratumorally and is associated with higher malignancy state [45]. On the other hand, according to recent studies, intratumoral expression of CCL5 may be induced by chemotherapy, favoring infiltration of effector T cells, thus providing a beneficial effect [46]. In support to this, we found that low levels of *Ccl5* coincided with low numbers of infiltrating CD8<sup>+</sup> T cells and with higher tumor aggressiveness. The controversial effect of CCL5 in recruiting cells with either immunosuppressive or antitumor functions is probably dictated by tumor microenvironment elements, further supporting the need of applying combinatorial research and treatment approaches.

Last but not least, our findings showed that more aggressive tumors were characterized with low levels of *Tnf- $\alpha$*  expression. In support to this, it has been previously reported that TNF- $\alpha$  has a major impact on the tumor-associated vasculature by inducing endothelial cell death, resulting in tumor regression, especially when combined with chemotherapy [47]. In addition, TNF- $\alpha$  exerts antitumor activity through activation of NK and CD8<sup>+</sup> T cells [48] as well as via induction of apoptosis [49]. On the other hand, TNF- $\alpha$  is considered a major pro-inflammatory cytokine, promoting carcinogenesis through inflammation [50]. Hence, this complex and contradictory role of TNF- $\alpha$  requires further investigation.

We could not detect any correlations between *Tgf- $\beta$* , *Ido* and *Arg* levels and tumor aggressiveness. However, the strong correlations observed between *Arg* and *Ido* levels with leukocytes infiltration could be explained by the previous studies describing their production by tumor-associated macrophages and infiltrating Tregs, respectively [51, 52].

Overall, the results presented herein should be considered as hypothesis-generating given the use of one parental cell line and the relatively small number of animals. Although the immune signatures described in the current study need further clarification, they are supportive to reports describing the important role of the intratumoral immunologic network in the control of tumor growth. Confirmation of these signatures, including immune-related genes and T cell infiltration in relation to growth characteristics, may also pave the way for the design of novel modalities targeting products of the relevant genes and thus optimizing the effectiveness of therapies in melanoma.

#### Compliance with ethical standards

**Conflict of interest** The authors declare that they have no conflict of interest.

#### References

- Ennen M, Keime C, Kobi D, Mengus G, Lipsker D, Thibault-Carpentier C, Davidson I (2015) Single-cell gene expression signatures reveal melanoma cell heterogeneity. *Oncogene* 34(25):3251–3263. doi:10.1038/onc.2014.262
- Kunz M (2016) Tumor heterogeneity, clonality and single cells. *Exp Dermatol* 25(11):857–858. doi:10.1111/exd.13092
- Hugo W, Shi H, Sun L, Piva M, Song C, Kong X, Moriceau G, Hong A, Dahlman KB, Johnson DB, Sosman JA, Ribas A, Lo RS (2015) Non-genomic and immune evolution of melanoma acquiring MAPKi resistance. *Cell* 162(6):1271–1285. doi:10.1016/j.cell.2015.07.061
- Li FZ, Dhillon AS, Anderson RL, McArthur G, Ferrao PT (2015) Phenotype switching in melanoma: implications for progression and therapy. *Front Oncol* 5:31. doi:10.3389/fonc.2015.00031
- Shannan B, Perego M, Somasundaram R, Herlyn M (2016) Heterogeneity in melanoma. *Cancer Treat Res* 167:1–15. doi:10.1007/978-3-319-22539-5\_1
- Hadrup S, Donia M, Thor Straten P (2013) Effector CD4 and CD8 T cells and their role in the tumor microenvironment. *Cancer Microenviron* 6(2):123–133. doi:10.1007/s12307-012-0127-6
- Botti G, Cerrone M, Scognamiglio G, Anniciello A, Ascierto PA, Cantile M (2013) Microenvironment and tumor progression of melanoma: new therapeutic perspectives. *J Immunotoxicol* 10(3):235–252. doi:10.3109/1547691X.2012.723767
- Gajewski TF, Schreiber H, Fu YX (2013) Innate and adaptive immune cells in the tumor microenvironment. *Nat Immunol* 14(10):1014–1022. doi:10.1038/ni.2703
- Rajkumar S, Watson IR (2016) Molecular characterisation of cutaneous melanoma: creating a framework for targeted and immune therapies. *Br J Cancer* 115(2):145–155. doi:10.1038/bjc.2016.195
- Clarke LE, Warf MB, Flake DD 2nd, Hartman AR, Tahan S, Shea CR, Gerami P, Messina J, Florell SR, Wenstrup RJ, Rushton K, Roundy KM, Rock C, Roa B, Kolquist KA, Gutin A, Billings S, Leachman S (2015) Clinical validation of a gene expression signature that differentiates benign nevi from malignant melanoma. *J Cutan Pathol* 42(4):244–252. doi:10.1111/cup.12475
- Galon J, Fox BA, Bifulco CB, Masucci G, Rau T, Botti G, Marincola FM, Ciliberto G, Pages F, Ascierto PA, Capone M (2016) Immunoscore and immunoprofiling in cancer: an update from the melanoma and immunotherapy bridge 2015. *J Transl Med* 14:273. doi:10.1186/s12967-016-1029-z
- Jonsson G, Busch C, Knappskog S, Geisler J, Miletic H, Ringner M, Lillehaug JR, Borg A, Lonning PE (2010) Gene expression profiling-based identification of molecular subtypes in stage IV melanomas with different clinical outcome. *Clin Cancer Res* 16(13):3356–3367. doi:10.1158/1078-0432.CCR-09-2509
- Harbst K, Staaf J, Lauss M, Karlsson A, Masback A, Johansson I, Bendahl PO, Vallon-Christersson J, Torngren T, Ekedahl H, Geisler J, Hoglund M, Ringner M, Lundgren L, Jirstrom K, Olsson H, Ingvar C, Borg A, Tsao H, Jonsson G (2012) Molecular profiling reveals low- and high-grade forms of primary melanoma. *Clin Cancer Res* 18(15):4026–4036. doi:10.1158/1078-0432.CCR-12-0343
- Foth M, Wouters J, de Chaumont C, Dynodot P, Gallagher WM (2016) Prognostic and predictive biomarkers in melanoma: an update. *Expert Rev Mol Diagn* 16(2):223–237. doi:10.1586/14737159.2016.1126511
- Griewank KG (2016) Biomarkers in melanoma. *Scand J Clin Lab Invest* 76(suppl245):S104–S112. doi:10.1080/00365513.2016.1210336
- Roesch A, Paschen A, Landsberg J, Helfrich I, Becker JC, Schandorf D (2016) Phenotypic tumour cell plasticity as a resistance mechanism and therapeutic target in melanoma. *Eur J Cancer* 59:109–112. doi:10.1016/j.ejca.2016.02.023
- Fortis SP, Anastasopoulou EA, Voutsas IF, Baxevas CN, Perez SA, Mahaira LG (2017) Potential prognostic molecular signatures in a preclinical model of melanoma. *Anticancer Res* 37(1):143–148. doi:10.21873/anticancer.11299
- Fidler IJ (1995) Melanoma metastasis. *Cancer Control* 2(5):398–404
- Balch CM, Gershenwald JE, Soong SJ, Thompson JF, Atkins MB, Byrd DR, Buzaid AC, Cochran AJ, Coit DG, Ding S, Eggermont AM, Flaherty KT, Gimotty PA, Kirkwood JM, McMasters KM, Mihm MC Jr, Morton DL, Ross MI, Sober AJ, Sondak VK (2009) Final version of 2009 AJCC melanoma staging and classification. *J Clin Oncol* 27(36):6199–6206. doi:10.1200/JCO.2009.23.4799
- Lundholm M, Hagglof C, Wikberg ML, Stattin P, Egevad L, Bergh A, Wikstrom P, Palmqvist R, Edin S (2015) Secreted factors from colorectal and prostate cancer cells skew the immune response in opposite directions. *Sci Rep* 5:15651. doi:10.1038/srep15651
- Elias EG, Hasskamp JH, Sharma BK (2010) Cytokines and growth factors expressed by human cutaneous melanoma. *Cancers (Basel)* 2(2):794–808. doi:10.3390/cancers2020794
- Zamarron BF, Chen W (2011) Dual roles of immune cells and their factors in cancer development and progression. *Int J Biol Sci* 7(5):651–658
- Fidler IJ (1973) Selection of successive tumour lines for metastasis. *Nat New Biol* 242(118):148–149
- Fidler IJ, Gersten DM, Budmen MB (1976) Characterization in vivo and in vitro of tumor cells selected for resistance to syngeneic lymphocyte-mediated cytotoxicity. *Cancer Res* 36(9 pt.1):3160–3165
- Hart IR (1979) The selection and characterization of an invasive variant of the B16 melanoma. *Am J Pathol* 97(3):587–600
- Fidler IJ, Kripke ML (1977) Metastasis results from pre-existing variant cells within a malignant tumor. *Science* 197(4306):893–895
- Poste G, Doll J, Brown AE, Tzeng J, Zeidman I (1982) Comparison of the metastatic properties of B16 melanoma clones isolated

- from cultured cell lines, subcutaneous tumors, and individual lung metastases. *Cancer Res* 42(7):2770–2778
28. Poste G, Doll J, Fidler IJ (1981) Interactions among clonal subpopulations affect stability of the metastatic phenotype in polyclonal populations of B16 melanoma cells. *Proc Natl Acad Sci USA* 78(10):6226–6230
  29. Mittal D, Gubin MM, Schreiber RD, Smyth MJ (2014) New insights into cancer immunoediting and its three component phases—elimination, equilibrium and escape. *Curr Opin Immunol* 27:16–25. doi:10.1016/j.coi.2014.01.004
  30. Whiteside TL (2008) The tumor microenvironment and its role in promoting tumor growth. *Oncogene* 27(45):5904–5912. doi:10.1038/onc.2008.271
  31. Landskron G, De la Fuente M, Thuwajit P, Thuwajit C, Hermoso MA (2014) Chronic inflammation and cytokines in the tumor microenvironment. *J Immunol Res* 2014:149185. doi:10.1155/2014/149185
  32. Voronov E, Carmi Y, Apte RN (2014) The role IL-1 in tumor-mediated angiogenesis. *Front Physiol* 5:114. doi:10.3389/fphys.2014.00114
  33. Lewis AM, Varghese S, Xu H, Alexander HR (2006) Interleukin-1 and cancer progression: the emerging role of interleukin-1 receptor antagonist as a novel therapeutic agent in cancer treatment. *J Transl Med* 4:48. doi:10.1186/1479-5876-4-48
  34. Swaika A, Hammond WA, Joseph RW (2015) Current state of anti-PD-L1 and anti-PD-1 agents in cancer therapy. *Mol Immunol* 67(2 Pt A):4–17. doi:10.1016/j.molimm.2015.02.009
  35. Itakura E, Huang RR, Wen DR, Paul E, Wunsch PH, Cochran AJ (2011) IL-10 expression by primary tumor cells correlates with melanoma progression from radial to vertical growth phase and development of metastatic competence. *Mod Pathol* 24(6):801–809. doi:10.1038/modpathol.2011.5
  36. Emmerich J, Mumm JB, Chan IH, LaFace D, Truong H, McClanahan T, Gorman DM, Oft M (2012) IL-10 directly activates and expands tumor-resident CD8(+) T cells without de novo infiltration from secondary lymphoid organs. *Cancer Res* 72(14):3570–3581. doi:10.1158/0008-5472.CAN-12-0721
  37. Moynihan KD, Opel CF, Szeto GL, Tzeng A, Zhu EF, Engreitz JM, Williams RT, Rakhra K, Zhang MH, Rothschilds AM, Kumari S, Kelly RL, Kwan BH, Abraham W, Hu K, Mehta NK, Kauke MJ, Suh H, Cochran JR, Lauffenburger DA, Wittrup KD, Irvine DJ (2016) Eradication of large established tumors in mice by combination immunotherapy that engages innate and adaptive immune responses. *Nat Med* 22(12):1402–1410. doi:10.1038/nm.4200
  38. Andersen MH, Schrama D, Thor Straten P, Becker JC (2006) Cytotoxic T cells. *J Invest Dermatol* 126(1):32–41. doi:10.1038/sj.jid.5700001
  39. Lavi G, Voronov E, Dinarello CA, Apte RN, Cohen S (2007) Sustained delivery of IL-1 Ra from biodegradable microspheres reduces the number of murine B16 melanoma lung metastases. *J Control Release* 123(2):123–130. doi:10.1016/j.jconrel.2007.07.015
  40. Goswami R, Kaplan MH (2011) A brief history of IL-9. *J Immunol* 186(6):3283–3288. doi:10.4049/jimmunol.1003049
  41. Parrot T, Allard M, Oger R, Benlalam H, Raingeard de la Bletiere D, Coutolleau A, Preisser L, Desfrancois J, Khammari A, Dreno B, Labarriere N, Delneste Y, Guardiola P, Gervois N (2016) IL-9 promotes the survival and function of human melanoma-infiltrating CD4(+) CD8(+) double-positive T cells. *Eur J Immunol* 46(7):1770–1782. doi:10.1002/eji.201546061
  42. Smith SE, Hoelzinger DB, Dominguez AL, Van Snick J, Lustgarten J (2011) Signals through 4-1BB inhibit T regulatory cells by blocking IL-9 production enhancing antitumor responses. *Cancer Immunol Immunother* 60(12):1775–1787. doi:10.1007/s00262-011-1075-6
  43. Kleffel S, Posch C, Barthel SR, Mueller H, Schlapbach C, Guenova E, Elco CP, Lee N, Juneja VR, Zhan Q, Lian CG, Thomi R, Hoetzenecker W, Cozzio A, Dummer R, Mihm MC Jr, Flaherty KT, Frank MH, Murphy GF, Sharpe AH, Kupper TS, Schatton T (2015) Melanoma cell-intrinsic PD-1 receptor functions promote tumor growth. *Cell* 162(6):1242–1256. doi:10.1016/j.cell.2015.08.052
  44. Black M, Barsoum IB, Truesdell P, Cotechini T, Macdonald-Goodfellow SK, Petroff M, Siemens DR, Koti M, Craig AW, Graham CH (2016) Activation of the PD-1/PD-L1 immune checkpoint confers tumor cell chemoresistance associated with increased metastasis. *Oncotarget* 7(9):10557–10567. doi:10.18632/oncotarget.7235
  45. Aldinucci D, Colombatti A (2014) The inflammatory chemokine CCL5 and cancer progression. *Mediators Inflamm* 2014:292376. doi:10.1155/2014/292376
  46. Hong M, Puaux AL, Huang C, Loumagne L, Tow C, Mackay C, Kato M, Prevost-Blondel A, Avril MF, Nardin A, Abastado JP (2011) Chemotherapy induces intratumoral expression of chemokines in cutaneous melanoma, favoring T-cell infiltration and tumor control. *Cancer Res* 71(22):6997–7009. doi:10.1158/0008-5472.CAN-11-1466
  47. Brouckaert P, Takahashi N, van Tiel ST, Hostens J, Eggermont AM, Seynhaeve AL, Fiers W, ten Hagen TL (2004) Tumor necrosis factor-alpha augmented tumor response in B16BL6 melanoma-bearing mice treated with stealth liposomal doxorubicin (Doxil) correlates with altered Doxil pharmacokinetics. *Int J Cancer* 109(3):442–448. doi:10.1002/ijc.11703
  48. Prevost-Blondel A, Neuenhahn M, Rawiel M, Pircher H (2000) Differential requirement of perforin and IFN-gamma in CD8 T cell-mediated immune responses against B16.F10 melanoma cells expressing a viral antigen. *Eur J Immunol* 30(9):2507–2515. doi:10.1002/1521-4141(200009)30:9<2507:AID-IMMU2507>3.0.CO;2-V
  49. Showalter A, Limaye A, Oyer JL, Igarashi R, Kittipatarin C, Copik AJ, Khaled AR (2017) Cytokines in immunogenic cell death: applications for cancer immunotherapy. *Cytokine* 97:123–132. doi:10.1016/j.cyto.2017.05.024
  50. Balkwill F (2009) Tumour necrosis factor and cancer. *Nat Rev Cancer* 9(5):361–371. doi:10.1038/nrc2628
  51. Spranger S, Spaepen RM, Zha Y, Williams J, Meng Y, Ha TT, Gajewski TF (2013) Up-regulation of PD-L1, IDO, and T(regs) in the melanoma tumor microenvironment is driven by CD8(+) T cells. *Sci Transl Med* 5(200):200ra116. doi:10.1126/scitranslmed.3006504
  52. Tham M, Tan KW, Keeble J, Wang X, Hubert S, Barron L, Tan NS, Kato M, Prevost-Blondel A, Angeli V, Abastado JP (2014) Melanoma-initiating cells exploit M2 macrophage TGFbeta and arginase pathway for survival and proliferation. *Oncotarget* 5(23):12027–12042. doi:10.18632/oncotarget.2482